Accepted Manuscript

Distributed modular temperature-strain sensor based on optical fiber embedded in laminated composites

Pingyu Zhu, Xiaobo Xie, Xiaopeng Sun, Marcelo A. Soto

PII: S1359-8368(18)33044-0

DOI: https://doi.org/10.1016/j.compositesb.2018.12.078

Reference: JCOMB 6407

To appear in: *Composites Part B*

Received Date: 14 September 2018

Revised Date: 15 December 2018

Accepted Date: 17 December 2018

Please cite this article as: Zhu P, Xie X, Sun X, Soto MA, Distributed modular temperature-strain sensor based on optical fiber embedded in laminated composites, *Composites Part B* (2019), doi: https://doi.org/10.1016/j.compositesb.2018.12.078.

Distributed modular temperature-strain sensor based on optical fiber embedded in laminated composites

Pingyu Zhu[1,2], Xiaobo Xie[1], Xiaopeng Sun[1], Marcelo A. Soto[1,3*]

[1] School of Mechanical and Electrical Engineering, Guangzhou University, 510060 Guangzhou, China

[2] EPFL Swiss Federal Institute of Technology, Institute of Electrical Engineering, SCI STI LT, Station 11, CH-1015 Lausanne, Switzerland

[3] Department of Electronic Engineering, Universidad Técnica Federico Santa María, 2390123 Valparaíso, Chile

*Corresponding author: Marcelo A. Soto, e-mail: marcelo.sotoh@usm.cl

Abstract

A smart structure based on carbon fiber reinforced polymer (CFRP) embedding optical fibers is proposed for distributed sensing in structural health monitoring. The proposed CFRP package provides mechanical protection to the optical fiber, enables temperature-strain discrimination, and also facilitates the sensor's installation to secure reliable measurements. Experimental results verify a linear strain sensor response with temperature compensation, agreeing well with the response of strain gauges and the expected theoretical behavior. The smart structure can be used by gluing it on the surface of the monitored structure or by embedding it as one of the layers used during manufacturing big composite structures.

Keywords: A. Carbon fibre; A. Layered structures; B. Stress transfer; D. Mechanical testing; Distributed optical fiber sensors

1. Introduction

Carbon fiber reinforced polymers (CFRP) have been developed extensively during the last years thanks to big progresses in materials science and technology [1], finding a wide range of applications, for instance in manufacturing parts of structural components in aircrafts [2] and large offshore wind turbine blades [3]. Possible damage of these large-scale critical structures [5,6] has recently raised some concerns on their safety issues [7,8]. The use of sensors embedded into CFRP during the early stages of the structure design has become an interesting and effective strategy to monitor the health of big composite structures [9,10] for studying their properties during material development and in-service operational monitoring. In this context, fiber-optic sensing has been proved

as a highly compatible technology to be embedded into CFRP laminated structures [11,12], thus providing a reliable solution for real-time structural health monitoring (SHM) [13].

The most common fiber sensing technology for SHM is based on fiber Bragg gratings (FBGs) [12]. Nevertheless, the use of FBGs at discrete pre-defined positions results in areas that unfortunately remain unmonitored, especially over large structures. To cope with the need of monitoring vast areas of interest over big structures, the use of distributed optical fiber sensing technologies becomes highly attractive. This technology actually allows monitoring some given physical variables (e.g. strain) using a single optical fiber over tens of kilometers, thus enabling continuous distributed monitoring of large composite structures [14-16]. However, embedding a very small and brittle optical fiber inside CFRP structures is a time-consuming process [17,18], and, moreover, it typically results in very low survival rates. Therefore, the ability to successfully incorporate optical fibers within CFRP components will make the fiber and structural parts integrated as a whole, rather than being disaggregated objects. In fact, to meet the requirements of engineering practical applications, the optical fiber must be ideally embedded and protected in an effective packaging. Fortunately, CFRP laminates consist of several layers, which offer the possibility of combining optical fiber sensors into a single large component using co-curing technology [19, 20].

Note that the use of fiber sensors in the field of SHM is essential to detect fractures, deformations or disbonding of CFRP structures, being temperature a parameter of lower relevance. Unfortunately, most of fiber sensors suitable for SHM [21-23] are sensitive to both temperature and strain, leading in many cases to an unwanted cross-sensitivity between these two physical variables [24,25]. This is especially critical in environments with changeable temperature conditions (e.g. when operating in wind turbines or aircraft structures [26,27]). One of the easiest approaches used for strain-temperature discrimination is to adopt different hybrid sensing techniques, such as combining FBG sensors with other sensing methods [28]. However, difficulties in real-field scenarios to achieve continuous (distributed) temperature-strain discrimination have prevented further developments from using discrete sensing techniques. Another alternative is to combine different distributed sensing techniques, such as Raman and Brillouin scattering [29,30] or to use birefringent fibers in combination with Brillouin [31] or Rayleigh [32] distributed sensing. However, all those approaches result in a significant increase of the cost and complexity of the system compared to the use of traditional fiber sensing techniques.

In this paper, a novel unit/modular distributed sensing concept based on an optical fiber embedded into laminated composites is proposed for temperature and strain measurements. Embedding an optical fiber into a CFRP package can give the possibility to design specific optical fiber layouts, which can potentially allow for reliable temperature-strain discrimination over large composite structures. The concept is here introduced presenting a basic omega (Ω)-shaped sensing cell through three possible combinations to form sensors with different sensing optical fiber layouts. A single sensing unit sample with temperature-strain-temperature monitoring sections has been fabricated and experimentally investigated. Making use of a distributed fiber sensor based on optical frequency-domain reflectometry (OFDR), the temperature and strain responses of the embedded optical fiber have been characterized under different heating conditions and static loading tests. The CFRP sensing unit has been designed with an optical fiber embedded within compressed and loose sections, thus allowing for temperature and strain discrimination. After temperature compensation, the OFDR sensor shows to have a linear response with respect to the applied load and induced strain, allowing us also to retrieve a 2D map of the distributed strain over the entire CFRP package. The proposed smart thin CFRP sensing unit with embedded optical fibers offers significant advantages compared to other sensing technologies and has great potential for several future SHM applications in composite structures. Thus, for instance, it can be installed on the surface or even inserted into curing structure parts as one of the layers for simultaneous distributed temperature and strain sensing.

2. Sensing unit and extension tape concept

The sensing unit concept proposed in this paper consists of a rectangular CFRP structure embedding an optical fiber placed in a 2D plane. The fiber is embedded in a way such that the CFRP package can be considered formed by several sensing sections, each one allowing for either distributed temperature sensing or distributed temperature-strain sensing. The 2D layout of the embedded fiber and the dimension of the different sensing zones can be designed and customized based on specific applications. Figure 1 shows an example of a CFRP structure consisting of five sections: three temperature sensing zones (pink shaded areas) and two temperature-strain sensing zones (blue shaded areas). In this case, the structure can be seen as evolving from an omega (Ω) shape, which forms four arched parts (indicated within red circles in Fig. 1a) and five straight lines (indicated by blue boxes in Fig. 1a). Thus, this basic sensing unit, as illustrated in Fig. 1a, is composed of two straight sections (denoted as “S1”, “S2”) for strain sensing, and three sections (denoted as “T1”, “T2”, “T3”) for temperature sensing. All curved fiber segments must be cured loosely inside the CFRP packaging to allow for strain-free

distributed temperature sensing, while the main straight sections are sandwiched between the two prepregs and compressed tightly, enabling simultaneous strain and temperature sensing. It is then expected that by using the temperature information measured in the loose fiber sections, temperature-free distributed strain measurements could be retrieved along the straight fiber areas. An optical fiber segment with straight and curved sections is shown in Fig. 1b.

It must be mentioned that the flatten Ω-shaped basic sensing unit can be patterned in many different shapes. For instance, back-to-back (Fig. 1c), face-to-face (Fig. 1d), and sequential stacking (Fig. 1e) are three, out of many, possible more implementations. Note that if the fiber ports denoted as "I" and "O" are directly connected together, the module becomes a single sensing unit by itself. However, "O" and "I" can also be used to append different modules together, so that this sensing module can be continuously replicated to a long-band sensor as needed. Since the two ends of the sensing optical fiber are maintained close to each other (i.e. at the same side of the CFRP packaging), the fiber layout can be readily used in a loop configuration, as required by some fiber sensing technologies, such as distributed Brillouin fiber sensing techniques based in optical time-domain analysis [33].

3. Principle of distributed optical fiber sensing for SHM

Distributed optical fiber sensors make use of a conventional optical fiber as a distributed linear sensing element, and exploit the natural light scattering generated in the fiber [34], such as Rayleigh, Raman and Brillouin scattering, to interrogate the surrounding environment. Those scattering phenomena are sensitive to environmental variables, allowing for the interrogation of physical variables such as temperature and strain along the optical fiber. There exist basically two interrogation approaches, which are based on either optical time-domain reflectometry (OTDR) [35] or optical frequency-domain reflectometry (OFDR) [36]. The time-domain approach typically enables distributed sensing over of several tens of kilometers of optical fiber with spatial resolutions in the meter scale; whilst the frequency-domain approach allows for much better spatial resolutions (down to millimeter scale) but over a reduced sensing range.

In the field of SHM, distributed fiber sensors based on either Brillouin or Rayleigh scattering can be employed to monitor strain over large structures. In these two cases, the strain affecting the structure can be transferred to the sensing fiber, resulting in a spectral shift of the sensor response. However, Brillouin and Rayleigh scattering are

both sensitive not only to strain changes in the fiber but also to temperature variations [24,25], resulting in an unwanted cross-sensitivity that makes almost impossible to discriminate temperature from strain in a single fiber position. In general, the response of Brillouin and Rayleigh sensors $\Delta f(z)$, as a function of the fiber position z, can be written as:

$$\Delta f(z) = C_T \Delta T(z) + C_\varepsilon \Delta \varepsilon(z) \quad (1)$$

where $\Delta T(z)$ and $\Delta \varepsilon(z)$ represent the local temperature and strain changes, and C_T and C_ε are the temperature and strain coefficients of the sensor, respectively. In the case of a Brillouin sensor C_T = 1.05 MHz/K and C_ε = 0.04 MHz/με [31], whilst in a Rayleigh-based sensor C_T = 1.3 GHz/K and C_ε = 150 MHz/με [32].

Another important feature of distributed fiber sensors to be considered for SHM is the capability of performing dynamic strain measurements. Conventional Brillouin sensing techniques are typically limited to quasi-static measurements; and even though dedicated interrogation methods exist for fast dynamic Brillouin sensing [37], their implementation with sub-meter spatial resolution capabilities becomes challenging. Rayleigh-based OFDR techniques, on the other hand, can allow simultaneous mm-scale resolution and dynamic strain measurements up to a few hundred Hz range, within short sensing ranges [38]. These features make Rayleigh OFDR sensing an ideal technology for distributed sensing in SHM applications.

The CFRP package system proposed here for distributed sensing applications in SHM is a kind of module design with standard fiber jumper interfaces, which can make use of either Brillouin or Rayleigh sensing techniques independently. In particular, a Rayleigh OFDR distributed fiber sensor [38] is here used for validating the proposed smart composite structure using millimeter spatial resolution and an interrogation rate of several tens of Hz.

4. Sensing unit fabrication and characterization

4.1. Sensing unit sample preparation

As a proof-of-concept, a smart CFRP packaging has been here manufactured based on T700 carbon fiber prepregs, peel plies and Teflon rods. The used pre-impregnated (prepreg) tape has a unidirectional ply orientation, and therefore, in order to maximize the strain transfer, the sensing optical fiber has been embedded

along the same direction of the carbon fiber. This secures a tight attachment between the sensing optical fiber and carbon fiber laminates for efficient strain transfer and more reliable sensing.

Figure 2a shows the optical fiber layout which has been designed for this proof-of-concept experiment. This is similar to the face-to-face configuration in Fig. 1d; however, only half of the scheme in that figure has been inserted into CFRP for testing. The positioning of the optical fiber defines three sections in this case, denoted as A, B and C in Fig. 2a. Sections A and C correspond to areas where the optical fiber has remained loose inside the CFRP packaging, enabling strain-free temperature sensing; while the optical fiber in section B has been tightly pressed inside the carbon fiber laminates, enabling simultaneous temperature and strain sensing. Measurements in Sections A and C can then be used to compensate the temperature effect measured in Section B, thus obtaining temperature-independent strain measurements. Note that this approach is possible because in most of practical applications it is not expected to have sharp spatial temperature gradients over the CFRP belt, allowing for the temperature of the tightly glued fiber (Section B) to be reliably estimated by interpolation of the temperature of the adjacent loose fiber sections (Sections A and C). Note that this approach does not represent a real limitation of the proposed structure since the size of the segments can be suitably designed depending on the application and expected spatial temperature gradients over the CFRP belt sensor.

In order to prepare the CFRP packaging, two pieces of 1100 mm × 180 mm carbon fiber prepregs are used. The optical fiber inside Sections A and C is placed within two short Teflon rods and two pieces of release clothes, so that some space for the optical fiber is created between two plies of carbon fiber prepreg during CFRP hot pressing. The optical fiber within segments in these spaces remains free from adhesion, enabling temperature measurements with no impact of strain. On the other hand, the fiber segments in Section B are placed parallel to the direction of the carbon fibers using regular intervals, as illustrated in Fig. 2a. The optical fiber segments in Section A and C are bent with a reasonably large curvature radius to avoid large optical losses in the embedded fiber, which could affect the performance of the distributed sensing system. A single fabricated sample is used in the experiment, as shown in Fig. 2b. The details of the fiber layout embedded into the manufactured sample are illustrated in Fig. 2c. The interval between adjacent parallel optical fibers for strain measurements is 14 mm, thus covering a surface (Section B) for distributed strain sensing of 70 mm × 700 mm. At the two ends of the sample, each temperature sensing section (Sections A and C) covers an area of 175 mm × 150 mm, as the strain-free

optical fibers are placed covering a wider surface (40 mm more at each side due to the fiber curvature, as shown in Fig. 2c).

In order to fabricate the CFRP packaging used for testing and validation of the proposed structure, a carbon fiber prepreg is first laid on top of an aluminum foil and gently flattened. Two pieces of release cloth are then placed at the sections defined for temperature sensing (light gray areas on the left- and right-hand side of the CFRP packaging in Fig. 2c). A 20 m-long standard single-mode optical fiber is then embedded in repeated "S" shapes over the entire area destined for sensing, as shown in Fig. 2a. The optical fiber is carefully embedded to secure that fiber segments are located in straight and parallel lines within Section B (denoted as I, II, III, IV, V and VI in Fig. 2a), while U turns with large enough bending radius are placed on release clothes at both ends of the belt (marked as □, □, □, □, and □ in Sections A and C). While the optical fiber segments in Section B are temporarily fixed by a roller pressing, two Teflon rods are placed on a release cloth along both sides of the carbon fiber prepreg long edges (Sections A and C). Then, the curved fibers in Sections A and C are covered with another release cloth, while an upper carbon fiber prepreg is placed on top and flatten with a pressing roller to ensure that a uniform surface is obtained without bubbles. The last step is to hot press the entire structure at a constant temperature of 120°C on a hot-pressing machine for 30 minutes at a pressure of 0.08 MPa. The CFRP structure is then cooled down for other 30 minutes, keeping the same pressure as before. Note that in order to avoid uneven curing residual stress in the embedded optical fiber, a pre-designed fiber clamper is used to make the optical fiber in Section B always in a pre-stressed state during the whole hot pressing process. Note that this pre-strain does not affect the OFDR sensing measurements, since this technology only provides relative strain measurements, i.e. quantifies only the relative strain changes compared to the strain at a calibration condition.

The packaged optical fibers are then connectorized at both ends, thus allowing us not only to connect the structure to a distributed optical fiber sensor interrogator, but also to connect consecutive smart CFRP packages in a large composite structure. Indeed, the prepared sample with embedded optical fibers before hot press can also be considered as a new piece of "prepreg" (smart skin or middle layer) for co-curing applications with other structural composite components.

4.2 Experimental setup

The optical fiber embedded into the CFRP package has been interrogated by Rayleigh-based OFDR technique using the experimental layout shown in Fig. 3. The fabricated CFRP package has been affixed to a metallic cantilever beam by gluing the aluminum foil substrate to the surface of the beam. Different weighs are applied to one side of the cantilever beam to induce different strains over the CFRP. The base of the aluminum foil in the CFRP packaging provides a tight connection with the metallic cantilever, allowing for an efficient transfer of the strain induced by the cantilever bending into the CFRP packaging. Note that, the cantilever beam has a longitudinally-varying cross-section that secures the same strength, so that when a load is applied to one of the ends of the cantilever, a uniform strain is transferred to the entire CFRP package. This way, the same amount of strain is expected to be transferred to the six parallel optical fiber segments (within Section B), allowing for a reliable characterization of the strain response of the CFRP packaging with embedded optical fibers.

For this characterization, a Rayleigh OFDR distributed fiber sensor with a 5 mm spatial resolution has been used to interrogate the 20 m-long sensing fiber, thus providing about 4000 independent sensing points over the CFRP package (all arranged in a 2D plane over the structure). The dynamic sampling rate of the OFDR sensor is limited by our instrumentation to 100 Hz, thus enabling reliable dynamic strain monitoring with frequency components of up to 50 Hz. In addition, a traditional strain gauge has been placed in the cantilever beam in order to provide a reference measurement for comparison and for evaluating the design of the CFRP package. In order to characterize the thermal response of the CFRP package, thermocouples have also been inserted in the temperature segments (Sections A and C), for comparison with the OFDR temperature response.

4.3 Temperature response of CFRP-embedded optical fiber

A first experiment has been carried out to quantify the response of the OFDR sensor to temperature changes. For this, Sections A and C have been heated up to ~42°C, as indicated by the thermocouples placed next to the embedded optical fibers inside the CFRP package. The distributed temperature profile measured by the OFDR sensor is illustrated in Fig. 4, which shows a good agreement with the temperature values obtained by the conventional thermocouples (showing an average value of ~42°C).

It must be noted that the distributed temperature profile measured by the OFDR system corresponds to the temperature distribution inside the CFRP package, thus providing sufficient information to discriminate

temperature from strain in OFDR measurements. However, retrieving the external CFRP structure temperature may still require further investigation in order to account for the thermal response and thermal conductivity of composite material. This study however goes beyond the scope of this paper, in which knowing the internal CFRP temperature is enough to provide strain-temperature discrimination in Section B.

4.4 Strain response of CFRP-embedded optical fiber

Then, the strain response of the proposed smart sensing belt has been characterized by applying different loads to the cantilever beam, and measuring the OFDR distributed profile response. Fig. 5 shows the response of the OFDR sensor as a function of the linear position along the embedded optical fiber for different applied loads, ranging from 1 kg up to 11 kg. Note that since the OFDR response is very sensitive to temperature changes (even in the order of a few mK [25]) and measurements are obtained in different (consecutive) instants, temperature compensation has been performed to obtain reliable strain measurements. This compensation has been carried out using the OFDR frequency response of the fiber sections □, □, □, □, and □. Note that those fiber segments are only affected by temperature changes (since they are not compressed inside the CFRP packaging) and therefore variations in the OFDR response within those sections can be only associated to temperature changes, which are straightforwardly used along with Eq. (1) to compensate thermal drifts in the entire measured trace. Results in Fig. 5 demonstrate that the OFDR response is essentially the same for the six fiber segments affected by strain (I to VI). While, this behavior is expected due to the uniform strain distribution provided by the cantilever shape, it also demonstrates the existence of a uniform strain transfer from the CFRP package and to the embedded optical fibers used for sensing.

Figure 6a shows the OFDR strain response of the CFRP package as a function of the applied load. It must be pointed out that the value shown in the figure for each applied load corresponds to the mean strain value measured by the OFDR sensor within the fiber sections I to VI (i.e. the mean value calculated within longitudinal windows of 100 points centered in each respective fiber segment). A linear response of the embedded sensor can be verified as a function of the applied load, showing a load-to-strain conversion factor equal to 8.49 με/kg. In order to validate these measurements, a similar graph has been plotted in Fig. 6b using strain gauge measurements. Results indicate that strain gauges report a slightly higher load-to-strain conversion factor (equal to 8.85 με/kg). This slightly different behavior can be basically attributed to the attenuation of the CFRP material itself and to the adhesive between the cantilever and CFRP packaging, leading to fiber sensing

measurements with reduced load-to-strain factor; while the strain gauges are directly glued on the surface of the cantilever, securing slightly better strain transfer in this case. It is therefore important to further investigate better methods for attaching the CFRP package to the external structures in order to maximize the strain transfer from the monitored structure to the proposed CFRP package with embedded fibers.

Measurements obtained by the OFDR sensor and strain gauges have also been validated by comparing them with theoretical values. For this comparison, the bending-induced strain in the cantilever beam has been calculated as a function of the applied load using the following well-known expression [39]:

$$\varepsilon = \frac{6WL}{Ebh^2} \tag{2}$$

where W = mg is the applied weight in Newton (using loads ranging from m = 1 kg up to 11 kg, and g = 9.8 m/s^2), L = 1104.6 mm is the cantilever length, E = 200 GPa is Young's modulus of the metallic cantilever, b = 400 mm is the width of the cantilever fixed-end, and h = 9.5 mm is the thickness of the cantilever.

Table 1 compares the results obtained by the OFDR sensor and traditional strain gauges (average values) with the theoretical values. As described before, small discrepancies can be observed; however, they are in good agreement with the results reported in the literature [33], where these small differences are mainly attributed to the distinct load-to-strain factors determined by the gluing and positioning of the gauges and CFRP packaging. Note that Table I also shows the relative strain efficiency of the OFDR system compared to the theoretical and gauge measured values. Results indicate an average OFDR strain efficiency of ~94.6% and ~96.4% compared to theoretical and gauge values, respectively.

Table 1. Comparison between measured strain values using OFDR distributed fiber sensing and traditional strain gauges with respect to the theoretical values obtained from Eq. (2)

Load (kg)	Theoretical value (με)	Strain gauges (με)	CFRP package w/OFDR (με)	OFDR efficiency vs. Theoretical	OFDR efficiency vs. Gauges
1	9.00	8.7	8.35	92.77 %	95.98 %
3	26.99	26.6	25.58	94.78 %	96.17 %
5	44.98	44.8	43.20	96.04 %	96.43 %
7	62.98	61.2	59.74	94.86 %	97.61 %
9	80.97	80.1	77.34	95.52 %	96.55 %
11	98.96	97.4	92.90	93.88 %	95.38 %

4.5 Two-dimensional strain mapping

So far the distributed strain profile measured by the OFDR sensor has been shown as a function of the linear position along the sensing fiber. However, retrieving a 2D mapping of the distributed strain profile could be more meaningful, providing information more in agreement with the two dimensions of the CFRP structure. Using the acquired data and knowing the optical fiber layout embedded into the CFRP package, a 2D map of the distributed strain profile over the CFRP package has been obtained as shown in Fig. 7, when loading the cantilever with 9 kg. This simple and intuitive 2D presentation of the measurement (rather than just displaying data all along the entire sensing fiber) is of great importance for practical engineering applications. As expected, results illustrate a relatively uniform strain profile over the entire 2D strain sensing region (Section B), as expected from the uniform-strain cantilever used in the experiment, and verifying the uniform strain transferred to the embedded optical fibers. Results indeed validate the proposed structure as a single distributed strain sensor (unaffected by temperature) to be installed in critical places where a particular attention is required to obtain a 2D map of local strain variations.

6. Conclusion and discussion

In this paper, a novel smart modular structure embedding optical fibers inside a CFRP packaging has been proposed for temperature and strain sensing over large composite structures. The CFRP package provides protection to the sensing fiber for monitoring harsh environments; however, it also allows for temperature-strain discrimination by embedding the optical fiber in tight and loose sections within CFRP laminates. For illustrating the design philosophy of this new structure, an omega (Ω)-shaped basic sensing unit has been introduced along with the evolution of a modular unit expanded into three possible sensing optical fiber layouts. A basic sensing sample with temperature-strain-temperature monitoring functions has been fabricated and then experimentally evaluated, demonstrating a strain response matching the response of traditional strain gauges and the behavior expected from the theory.

It must be pointed out that the design of the optical fiber placement can be customized to the requirements of specific applications by designing the length, shape and covered area of the different sections of the embedded fiber. However, it is worth noting that the dimensions of the loose optical fiber sections must be carefully planned, since the wrong design of the tiny space between the two layers of carbon fibers might lead to structural

defects in some cases. In addition, the dynamic characteristics of the proposed smart structure are still subjects for future research.

It should be emphasized that the proposed smart CFRP structure can be used as a module that can be extended by continuously connecting more basic sensing modules during manufacture. Two ways of installing the proposed CFRP structure are envisage at this stage: *i)* to glue it on the surface of the structure to be monitored by choosing an appropriate substrate to achieve a good matching with the monitored structural material, and thus to increase the strain transfer to the CFRP package; *ii)* to insert it into the structure as one of the composite layers used during the manufacturing process. The smart modular structure embedding optical fibers can actually act as a real nervous system inside the structure, allowing for the monitoring of the strain and temperature changes experienced by the sensing substrate. This can indeed be considered as a relevant contribution to the field of SHM due to the unmatched features provided by the proposed smart CFRP belt, which cannot be achieved using conventional electronic sensors.

Acknowledgments

The authors would like to thank Prof. Luc Thévenaz and Mr. Desmond Chow from EPFL Swiss Federal Institute of Technology for the fruitful discussions in the early stages of this research. The authors also acknowledge the financial support of Science and Technology Fund of Guangdong Province, Grant No. 2016A010102020 and Science and Technology Fund of Guangzhou City, Grant No. 201504291326362.

References

1. Hofstätter T, Pedersen DB, Tosello G, Hansen HN. State of the Art of Fiber-Reinforced Polymers in Additive Manufacturing Technologies. J Reinf Plast Comp 2017; 36(15):1061-1073.
2. Hashish M and Kent WA. Trimming of CFRP aircraft components. In: WJTA-IMCA conference and Expo, Houston, UK, 2013.
3. Mishnaevsky L, Branner K, Petersen HN, Beauson J, McGugan M, Sørensen BF. Materials for wind turbine blades: an overview. Materials 2017; 10(11): 1-12.
4. Ou Y, Zhu D, Zhang H, Yao Y, Mobasher B, Huang L. Mechanical properties and failure characteristics of CFRP under intermediate strain rates and varying temperatures. Compos Part B 2016; 95:123-136.

5. Tenney DR, Davis JG Jr, Pipes RB, Johnston N. NASA Composite Materials Development: Lessons learned and future challenges. In: NATO RTO AVT-164 Workshop on support of composite systems. Bonn, October, Germany, 2009.
6. Sierra-Pérez J, Torres-Arredondo MA, Güemes A. Damage and nonlinearities detection in wind turbine blades based on strain field pattern recognition. FBGs, OBR and strain gauges comparison. Compos Struct 2016; 135:156–166.
7. Baker A, Dutton S, Kelly D. Composite materials for aircraft structures. AIAA: Reston, VA, USA, 2004.
8. Diamanti K, Soutis C. Structural health monitoring techniques for aircraft composite structures. Prog Aerosp Sci 2010; 46: 342-352.
9. Pfeiffer H, and Wevers M. Structural health monitoring and its implementation within the European project. In: EU project meeting on aircraft integrated structural health assessment (AISHA), Leuven, June, Belgium, 2007.
10. Grave JHL, Håheim ML, Echtermeyer AT. Evaluation of the strain field in a composite - metal adhesive joint with an optical backscatter reflectometer. In: Proceedings of the 15th European conference on composite material. Venice, Italy, 2012.
11. Di Sante R. Fibre optic sensors for structural health monitoring of aircraft composite structures: recent advances and applications. Sensors 2015; 15:18666-18713.
12. Slattery SA, Nikogosyan DN, Brambilla G. Fiber Bragg grating inscription by high intensity femtosecond UV laser light: Comparison with other existing methods of fabrication. J Opt Soc Am B 2005; 22: 354-361.
13. Cai J, Qiu L, Yuan S, Shi L, Liu P, Liang D. Structural health monitoring for composite materials. In Composites and Their Applications; InTech: Rijeka, Croatia, 2012.
14. Güemes A, Fernández-López A, Patricia F, Díaz-Maroto, Lozano A, Sierra-Perez J. Structural health monitoring in composite structures by fiber-optic sensors. Sensors 2018; 18:1094.
15. Vulliez P. Distributed fiber-optic sensing solves real-world problems. Laser focus world 2013; 49: 60-67.
16. Wild G, Hinckley S. Distributed optical fiber smart sensors for structural health monitoring. In Proceedings of the 8th international workshop on structural health monitoring, Stanford, USA, 2011, p.13-15.

17. Schroeder K, Ecke W, Apitz J, Lembke E, Lenschow G. A fibre Bragg grating sensor system monitors operational load in a wind turbine rotor blade. Meas Sci Technol 2006; 17: 1167-1172.
18. Kim SW, Kang WR, Jeong MS, Lee I, Kwon IB. Deflection estimation of a wind turbine blade using FBG sensors embedded in the blade bonding line. Smart Mater Struct 2013; 22:1-11.
19. Monaghan T, Capel AJ, Christie SD, Harris RA, Friel RJ. Solid-state additive manufacturing for meatallized optical fiber integration. Compos Part A-Appl S 2015; 76:181-193.
20. Rito RL, Crocombe AD, Ogin SL. Health monitoring of composite patch repairs using CFBG sensors: experimental study and numerical modeling. Compos Part A-Appl S 2017; 100: 255-268.
21. Minakuchi S, Banshoya H, Ii S, and Takeda N. Hierarchical fiber-optic delamination detection system for carbon fiber reinforced plastic structures. Smart Mater Struct 2012; 21:105008.
22. Nishio M, Muzutani T, Takeda N. Structural shape reconstruction with consideration of the reliability of distributed strain data from a Brillouin-scattering-based optical fiber sensor. Smart Mater Struct 2010; 19.
23. Barrias A, Casas J, Villalba S. A review of distributed optical fiber sensors for civil engineering applications. Sensors 2016; 16:748.
24. Horiguchi T, Shimizu K, Kurashima T, Tateda M, Koyamada Y. Development of a distributed sensing technique using Brillouin scattering. J Lightwave Technol 1995, 13(7):1296-1302.
25. Koyamada Y, Imahama M, Kubota K, Hogari K. Fiber-optic distributed strain and temperature sensing with very high measurand resolution over long range using coherent OTDR. J Lightwave Technol 2009; 27: 1142-1146.
26. Madsen S F, Carloni L. Lightning exposure of carbon fiber composites in wind turbine blades. 24th Nordic insulation symposium on materials, Components and Diagnostics. Copenhagen, June, 2015.
27. Choi K-S, Huh Y-H, Kwon I-B and Yoon D-J. A tip deflection calculation method for a wind turbine blade using temperature compensated FBG sensor. Smart Mater Struct 2012; 21:1-8.
28. Zaidi F, Nannipieri T, Soto MA, Signorini A, Bolognini G, Di Pasquale F. Integrated hybrid Raman/fiber Bragg grating interrogation scheme for distributed temperature and point dynamic strain measurements. Appl Opt 2012; 51:7268-7275.
29. Alahbabi MN, Cho YT, Newson TP. Simultaneous temperature and strain measurement with combined spontaneous Raman and Brillouin scattering. Opt Lett 2005; 30: 1276-1278.

30. Bolognini G, Soto MA, Di Pasquale F. Fiber-optic distributed sensor based on hybrid Raman and Brillouin scattering employing multi-wavelength Fabry-Pérot lasers. IEEE Photonic Tech L 2009; 21(20): 1523–1525.
31. Zou W, He Z, Hotate K. Complete discrimination of strain and temperature using Brillouin frequency shift and birefringence in a polarization-maintaining fiber. Opt Express 2009; 17(3): 1248-1255.
32. Lu X, Soto MA, Thévenaz L. Temperature-strain discrimination in distributed optical fiber sensing using phase-sensitive optical time-domain reflectometry. Opt Express 2017; 25:16059-16071.
33. Soto MA, and Thévenaz L, Modeling and evaluating the performance of Brillouin distributed optical fiber sensors. Opt Express 2013; 21(25): 31347–31366.
34. Boyd RW. Nonlinear Optical. 2nd ed. San Diego, CA - London: Academic Press, 2003.
35. Aoyama KI, Nakagawa K, Itoh T. Optical time domain reflectometry in a single-mode fiber. IEEE J Quantum Electron 1981; QE-17(6): 862-868.
36. Eickhoff W, Ulrich R. Optical frequency domain reflectometry in single‐mode fiber. Appl Phys Lett 1981; 39:693.
37. Motil A, Bergman A, Tur M. State of the art of Brillouin fiber-optic distributed sensing. Opt Laser Technol 2016; 78:81-103.
38. Froggatt ME, Gifford DK, Kreger S, Wolfe M, Soller BJ. Characterization of polarization-maintaining fiber using high-sensitivity optical-frequency-domain reflectometry. J Lightwave Technol 2006; 24(11):4149-4154.
39. Kwak SY, Hwang HY. Effect of heat treatment residual stress on stress behavior of constant stress beam. Journal of Computational Design and Engineering 2018; 5: 137-143.

Figures

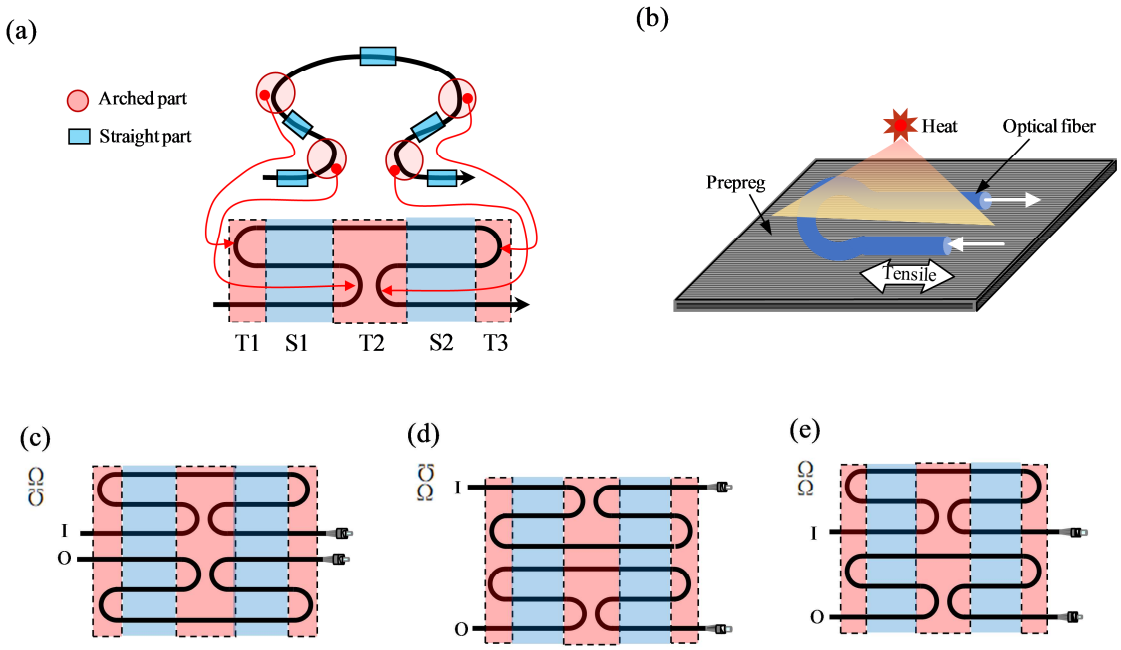

Figure 1. Schematic of proposed sensing unit. (a) Basic Ω-shaped fiber to be used to form the sensing structure. (b) Basic sensing cell for both temperature and strain measurements. (c) Back-to-back layout. (d) Face-to-face layout. (e) Sequential stacking layout.

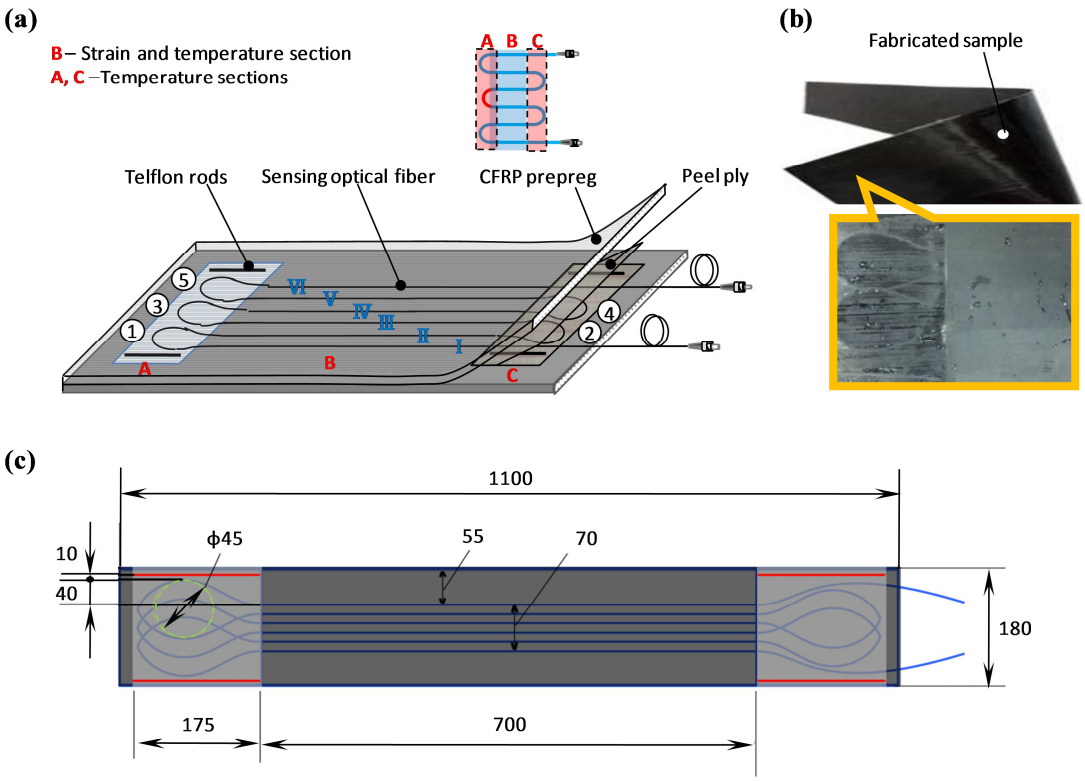

Figure 2. (a) Schematic of the CFRP packaging with embedded optical fibers for distributed sensing. (b) Fabricated modular CFRP structure. (c) Details of optical fiber layout.

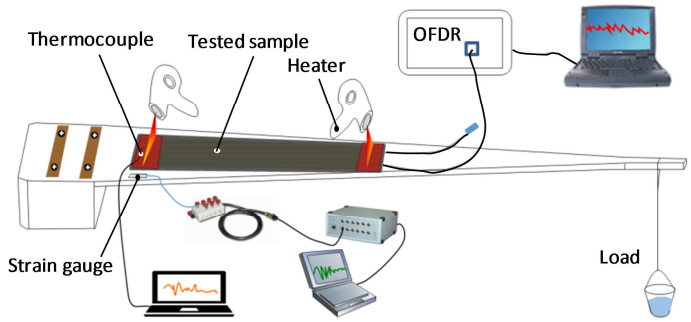

Figure 3. Schematic diagram of the strain sensing loading test.

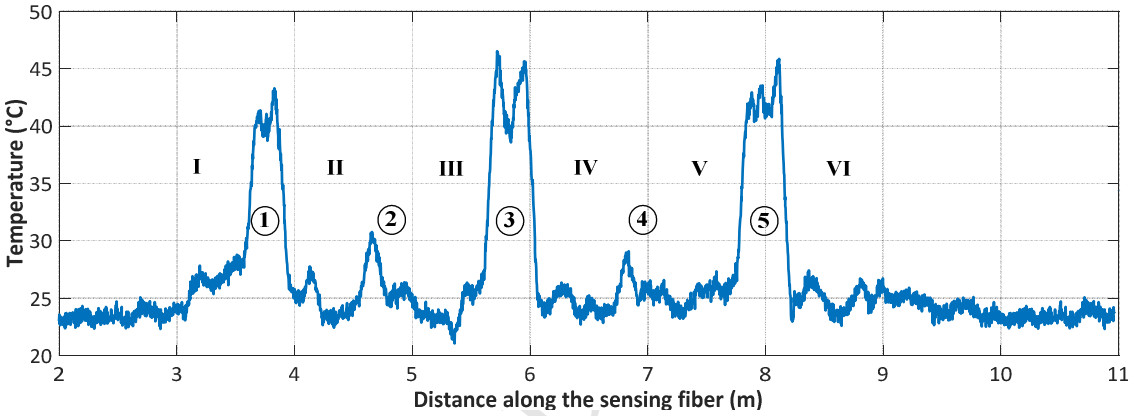

Figure 4. Experimental distributed OFDR temperature response of the CFRP packaging.

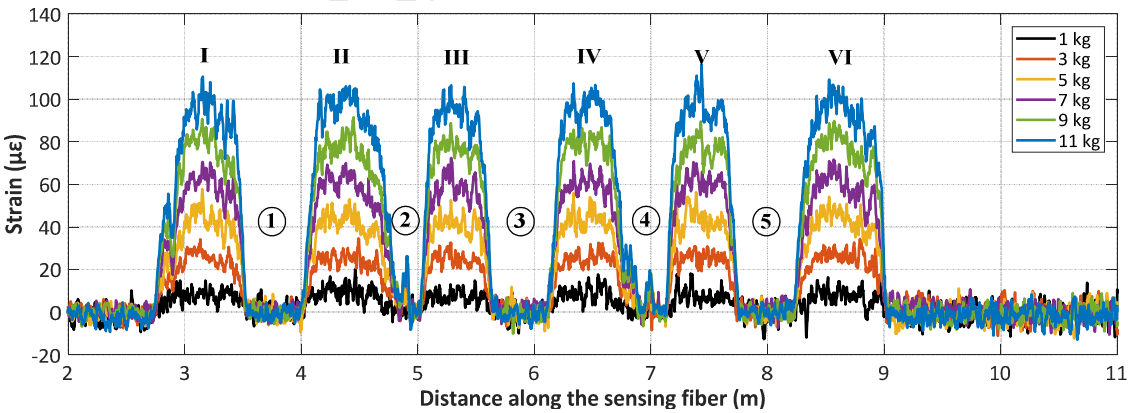

Figure 5. Experimental distributed OFDR strain response of the CFRP packaging for different loads.

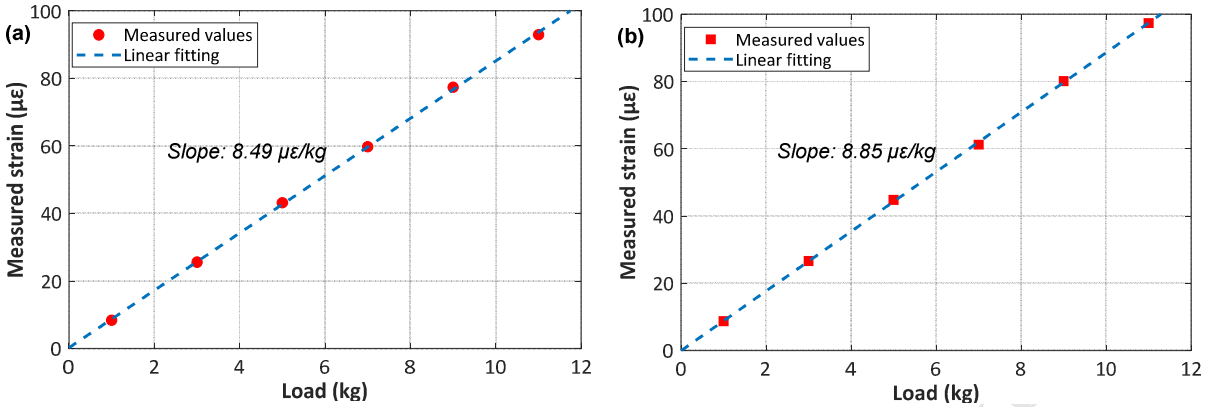

Figure 6. Measured (average) strain response versus applied load for (a) OFDR sensor with embedded optical fibers in the proposed CFRP packaging, and (b) conventional strain gauges.

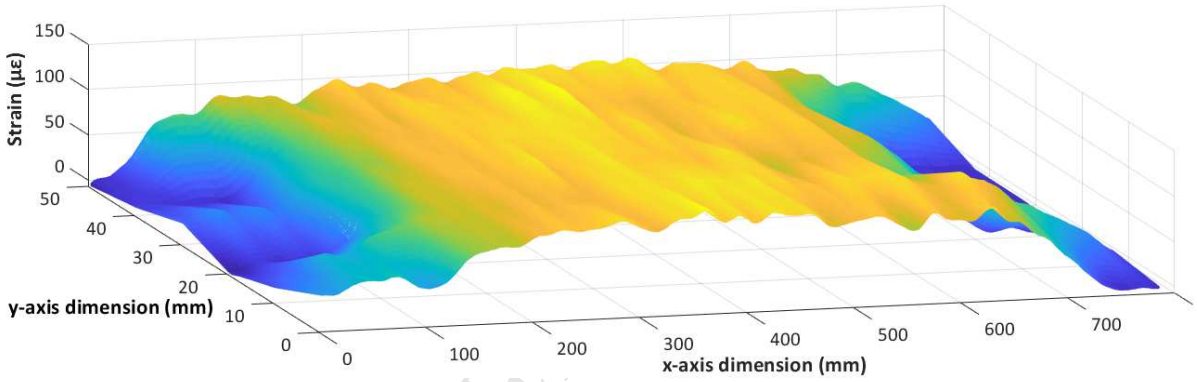

Figure 7. Retrieved 2D distributed strain profile measured on the CFRP package when the cantilever beam is loaded with 9 kg.